Title: Magnetization processes of irregular dendrite structures - a Monte Carlo study

Author: Grzegorz Ziółkowski, Artur Chrobak

Citation style: Ziółkowski Grzegorz, Chrobak Artur. (2020). Magnetization processes of irregular dendrite structures - a Monte Carlo study. "Physica B: Physics of Condensed Matter" (Vol. 577 (2020), art. no. 411745, s. 1-5), DOI:10.1016/j.physb.2019.411745

Physica B 577 (2020) 411745

Contents lists available at ScienceDirect

Physica B: Physics of Condensed Matter

journal homepage: http://www.elsevier.com/locate/physb

Magnetization processes of irregular dendrite structures - A Monte Carlo study

Grzegorz Ziółkowski [*], Artur Chrobak

Institute of Physics, University of Silesia in Katowice, 75 Pułku Piechoty 1A, 41-500, Chorzów, Poland

ARTICLE INFO

Keywords:
Monte Carlo simulations
Ultra-high coercive alloys
Diffusion limited aggregation

ABSTRACT

The paper refers to micromagnetic simulations of magnetization processes of dendrite-like object. The objects were generated by the DLA fractal algorithm that allows obtaining fractals with different ratio of the spins attributed to the surface to volume. The simulations were carried out using the cluster Monte Carlo algorithm designed for spin continuous and multiphase magnetic systems. The presented researches include different magnetic anisotropy of the surface and volume reflected magnetically soft, hard and ultra-high coercive phases. As it was shown, the influence of microstructure on the coercivity mechanism is a complex phenomenon. In the case of the fractals with magnetically soft volume the increasing surface contribution causes either increse or decrease of the coercive field for relatively high or low magnetic anisotropy of the surface, respectively. For the fractals with ultra-high coercive volume the occurrence of the surface anisotropy leads to the significant deterioration of their hard magnetic properties. The obtained spin configurations show that this effect is related to non-colinear directions of the surface anisoropy and strong enough exchange coupling between the surface and volume.

1. Introduction

Magnetic materials are very important in nowadays technologies. New and continuously increasing requirements of high-effective magnets can be fulfilled by modern nanostructured magnetic composites containing phases characterized by different magnetic properties. In the field of permanent magnets, especially interesting are new magnetic materials without or with a reduced content of rare earth elements [1,2] which is the main research direction in the area of the so-called hard magnets. It seems that nanomaterials, especially powders and composites, can bring the desired results [3–5]. Recently, we have reported unique hard magnetic properties of Tb–Fe–B–Nb bulk alloys, i.e. coercive field over 8 T at room temperature [6,7]. An example of hysteresis loops for the $(Fe_{80}Nb_6B_{14})_{0.88}Tb_{0.12}$ alloy is presented in Fig. 1. This alloy was obtained using the vacuum suction casting method in a form of bulk rod. As shown in our previous works [6,7], the ultra-high coercivity is attributed to a dendritic microstructure of $Tb_2Fe_{14}B$ grains (see the SEM image in Fig. 1). Formation of the specific microstructure was possible by a combination of the proper Nb content and the cooling rate during casting. In the Tb–Fe–B system, magnetic moments of Tb and Fe are coupled antiferromagnetically which is responsible for relatively low magnetic remanence ($\mu_0M_r \approx 0.3$ T) as well as $|BH|_{max}$ (about 13 kJ/m^3). However, the Fe–Nb–B–Tb bulk alloys can be considered as material with extremely high resistance to external magnetic field, and therefore, their particles can be a source of magnetic anisotropy in powders as well as bulk composites containing magnetically soft and the ultra-high coercive phases. The high coercivity is a unique feature in the case of bulk alloys, and therefore, researches concerning magnetization processes of such materials are of great importance. In this field, simulations of dendritic systems can be very useful for understanding origin of the unique magnetic properties, including an impact of microstructure on their coercivity mechanism [8–10].

In the present work we carried out Monte Carlo studies concerning irregular dendritic structures of soft and hard magnetic phases embedded into non-magnetic matrix. The dendritic structure was generated using the so-called diffusion limited aggregation (DLA) algorithm, allowing modeling a wide range of dendritic or dendrite-like microstructures characterized by different volume to surface ratio. The main goal of our simulations is to study magnetization processes of the DLA-generated objects characterized by different magnetic properties of the volume and surface, including the magnetically soft and ultra-high coercive phases.

---

[*] Corresponding author.
E-mail address: grzegorz.ziolkowski@us.edu.pl (G. Ziółkowski).

https://doi.org/10.1016/j.physb.2019.411745
Received 30 June 2019; Received in revised form 17 August 2019; Accepted 3 October 2019

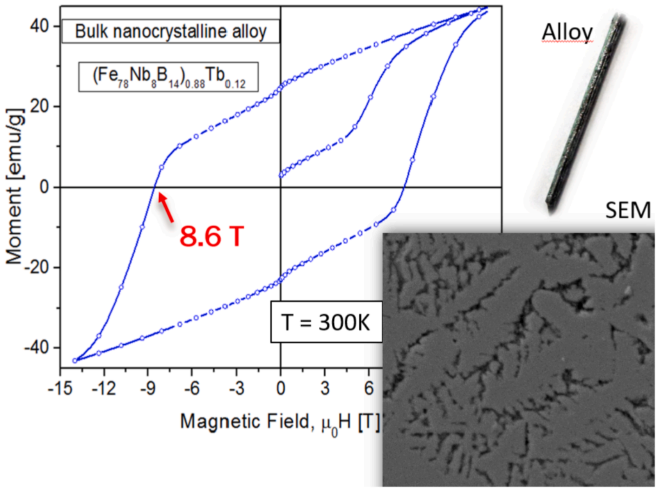

Fig. 1. Example of Tb–Fe–B–Nb bulk nanocrystalline alloy, its magnetic hysteresis loop as well as a specific dendritic-like microstructure observed by SEM technique.

2. Simulation procedure

Magnetization processes were simulated using the modified cluster Monte Carlo algorithm. This approach was developed by our team and presented in Ref. [11]. The main improvement relies in the cluster detection procedure. The procedure is not only dependent on the exchange coupling and the thermal energy (like in the classical cluster algorithms) [12,13] but also it is sensitive to disorder of magnetic properties typical for multiphase systems. The simulation procedure consists of series of Monte Carlo (MC) steps and it is very similar to the classical Metropolis algorithm designed for continuous spin systems. The main idea of the single iteration can be summarized as follows:

1. Chose a random node *i* in the spins system.
2. With the probability 1 - $P_{\rm cl}$ change the spin $S_{\rm i}$ direction by the θ angle and go to step 4.
3. Find a cluster around spin $S_{\rm i}$ and change cluster spins directions by θ angle.
4. Calculate the system energy difference ΔE before and after the change. Accept the change and go to step 1 with the probability $exp\left(\frac{-\Delta E}{k_B T}\right)$.
5. Otherwise, restore the previous configuration and go to step 1.

Energy of the system is computed in the frame of the 3-D Heisenberg model:

$$E = -\sum_{i,j} J_{ij} S_i \cdot S_j - \sum_i K_i (S_i \cdot n_i)^2 - g\mu_B \mu_0 \sum_i H_i \cdot S_i$$
$$+ D\sum_{i,j} \frac{S_i \cdot S_j - 3(S_i \cdot e_{ij})(S_j \cdot e_{ij})}{r_{ij}^3}$$

where $\underline{J}_{\rm ij}$ is the exchange parameter, $S_{\rm i}$ is the spin vector on site *i*, $K_{\rm i}$ is the anisotropy constant (per site), $n_{\rm i}$ is the easy magnetization axis, g is the Lande factor, $\mu_{\rm B}$ is the Bohr magneton, μ_0 is the vacuum permeability and $H_{\rm i}$ is the magnetic field on site *i*, *D* is the dipolar constant, $e_{\rm ij}$ is the directional versor between the *i*-th and *j*-th nodes, $r_{\rm ij}$ is the distance between the *i*-th and *j*-th nodes. Note, that the described procedure is repeated $N_{\rm iter}$ times for each MC step and the average spin in the external field direction $<S_z>$ is calculated based on $N_{\rm step}$ steps.

The key point in the simulation is the cluster building procedure which, like in the classical algorithms, utilizes the so-called adding probability $P_{\rm add} = 1\text{-exp}(-E_{\rm coupling}/k_B T)$ where $E_{ij}^{coupling}$ is the direct exchange coupling energy between the nodes *i* and *j*. This probability is decreased by an additional factor attributed to a local configuration entropy $S_i^{\rm loc}$ of some properties (in our case, magnetic anisotropy *K*) calculated in the defined sphere around the *i*-th node, for details see Ref. [11].

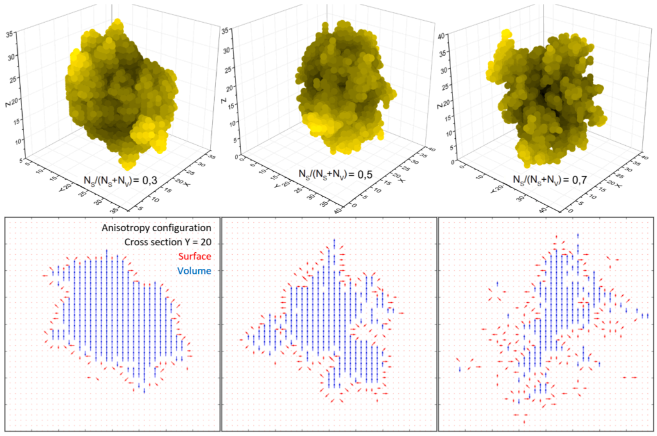

Fig. 2. Three type of simulated systems with differed number of spins on the surface and in the volume as well as cross section for this systems.

In this work, five types of systems (40 × 40 × 40 nodes) were generated based on the DLA method [14–18]. Each of them are different in a degree of a branch extension, and consequently, in the ratio of the number of spins on the surface to the whole object, i.e. $N_{\rm S}/(N_S + N_{\rm V})$ equal to 0.3, 0.4, 0.5, 0.6 and 0.7. The exemplary studied systems are presented in Fig. 2 as a 3D view as well as a 2D cross-section through the center. The spins on the surface (marked in red) are characterized by surface anisotropy K_S equal to 0, 5e-4 and 5e-3 eV and spins in the volume (marked in blue) are characterized by volume anisotropy $K_{\rm V}$ equal to 0, 5e-5 and 5e-4 eV. In addition, note that the direction of the $K_{\rm V}$ anisotropy has been set in the z-axis direction (in the figures vertically), while the surface anisotropy takes the normal vector direction (perpendicular to the surface) calculated individually for each spin.

The values of the main simulation parameters have been set at: $k_B T = 1\text{e-}5$ eV, D = 1.8 eV nm^3, $P_{\rm cl} = 1\text{e-}3$, $\theta = \pi/100$, $J = 1.5\text{e-}2$ eV, $N_{\rm loop} = 192\,000$ and $N_{\rm iter} = 400$ for the temperature of the system, dipolar constant (resulting from the physical value of dipolar interaction energy between spins $S = 1$ and distance 1 nm), probability of cluster analysis, spin direction change, exchange parameter (corresponds to the Curie temperature of about 1000 K), number of loops in one MC iteration and number of iteration for magnetization averaging, respectively. For simplicity, the spin vector length equals 1 for the both volume and surface. The values of the initial parameters were chosen according to our experience on micromagnetic MC simulations with the modified cluster algorithm.

3. Results and discussion

In order to study magnetization processes and coercivity mechanism of the dendrite-like objects, a set of the-so-called reverse magnetization curves was simulated. Particularly, the spins directions were initially placed in the *z*-axis direction which is attributed to full magnetic saturation for enough high magnetic field H > 0. Next, the reverse magnetization curves were collected during a subsequent decrease of the external magnetic field by the 0.25 T step.

Fig. 3 shows the reverse magnetization curves for different combinations of surface and volume anisotropy values. The simulations were carried out for the five degrees of the DLA fractal development i.e. $N_{\rm S}/(N_S + N_{\rm V})$ equal to 0.3, 0.4, 0.5, 0.6 and 0.7. The values of the coercive fields for the systems with the specific $K_{\rm S}$ and $K_{\rm V}$ were completed in the form of charts in the $N_{\rm S}/(N_S + N_{\rm V})$ function, as shown in Fig. 4. From the

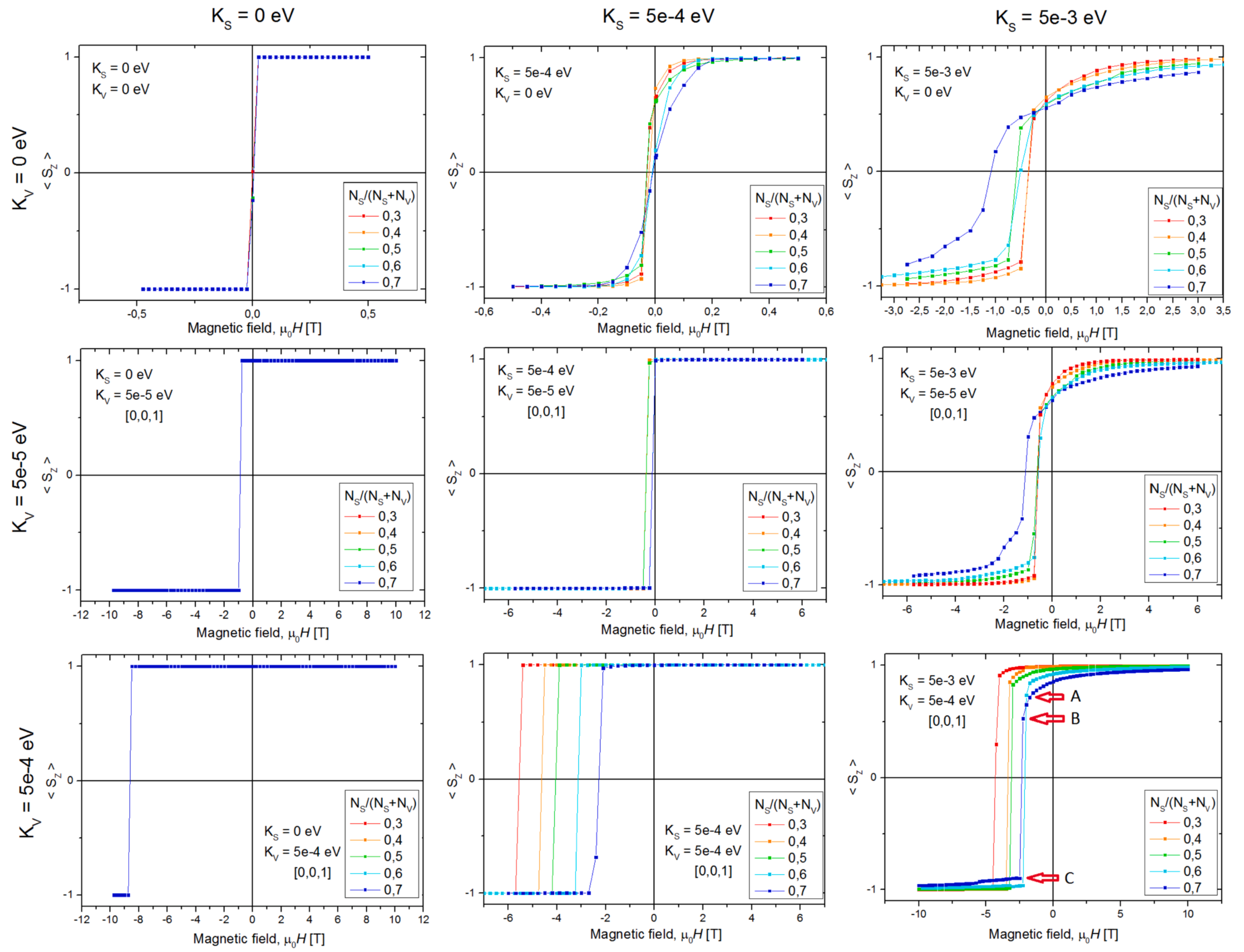

Fig. 3. The reverse magnetization carves for different combinations of surface and volume anisotropy value as well as the ratio between the spins on the surface and in the volume.

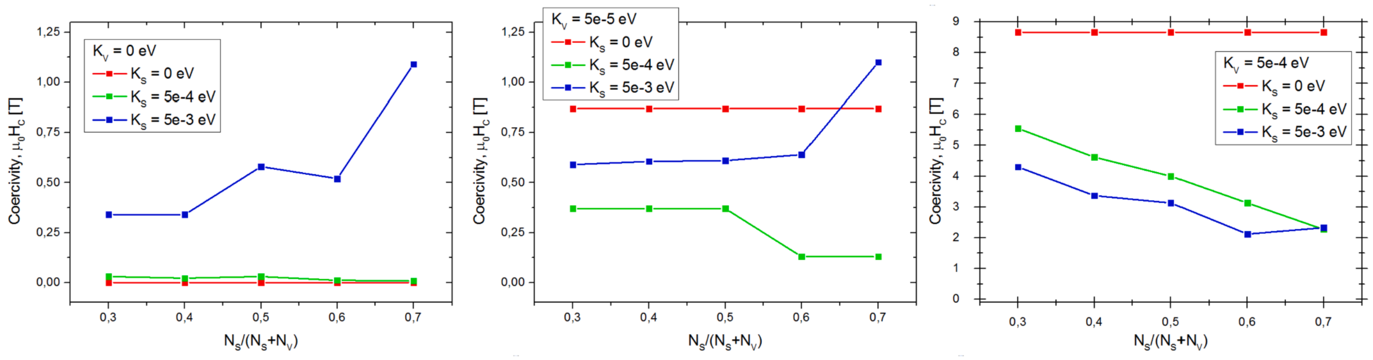

Fig. 4. The value of the coercive field for systems with specific K_S and K_V as a function of $N_S/(N_S + N_V)$.

first column in Fig. 3 ($K_S = 0$ eV) the reference coercivity of the volume can be detected as $H_C = 1$ T and 8.5 T for the $K_V = $ 5e-5 eV and 5e-4 eV, respectively. This means that the chosen values of the volumetric anisotropy well reflect magnetically hard and ultra-high coercive phases.

For the cases with $K_V = 0$, the introduction of the surface anisotropy leads to the observed magnetic hardening, i.e. increase of H_C. However, an increase of the surface contribution leads to a decrease of H_c for $K_S = $ 5e-4 eV while, for $K_S = $ 5e-3 eV one can see a significant increase of this parameter. The first effect is expected, taking in to account the fact that the low and disordered values of K_S cause averaging out of apparent magnetic anisotropy, like in the Herzer random anisotropy model of nanocrystalline soft magnetic systems [19]. Nevertheless, high enough value of K_S should result in magnetic hardening of the soft magnetic object, as observed in Figs. 3 and 4.

Different behavior was observed for the systems with higher than

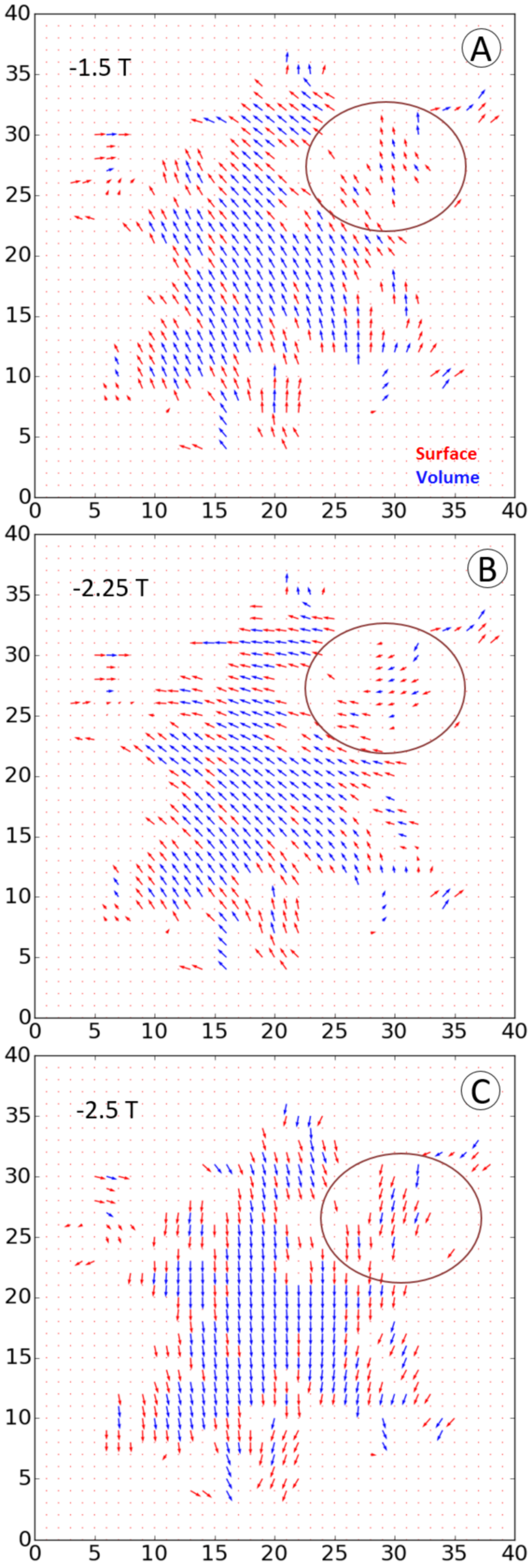

Fig. 5. The spin configurations in the cross-section (Y = 20) for the points of simulation which were marked in Fig. 3 (K_S = 5e-3 eV, K_V = 5e-4 eV and $N_S/(N_S + N_V) = 0.7$).

zero magnetic anisotropy of the volume. Generally, the occurrence of the surface anisotropy causes a deterioration in magnetic coercivity. This effect is particularly visible for the case of K_V = 5e-4 eV ($N_S/(N_S + N_V) = 0.7$) where H_C drops from 8.5 T to 2.2 T for $K_S = 0$ and K_S = 5e-4 eV, respectively.

This surprising result shows that not in all cases the higher surface anisotropy contributes to magnetic hardening of the volume. For better understanding the coercivity mechanism in such systems, it is worth to trace the spin configurations during the remagnetization process, as shown in Fig. 5 for K_S = 5e-3 eV, K_V = 5e-4 eV and $N_S/(N_S + N_V) = 0.7$. Note that the spins on the surface have anisotropy directed non-colinear to the direction of the external magnetic field. This means that a magnetostatic energy required for the reverse magnetization is lower in a comparison with the volume, where the anisotropy is parallel to the field. If the surface spins change their directions the volume spins can follow this new configuration via the exchange interactions. Finally, these effects can lead to significant decrease of the coercive field of the whole object dependently on K_S/K_V and $N_S/(N_S + N_V)$ ratio. In fact, the described scenario can be observed in Fig. 5 where the reverse magnetization process starts from the change of spin directions on the surface (see the spins in the circle).

The revealed effect can be very useful for designing magnetic composites containing the ultra-high coercive phases. For example, grinding of hard magnetic alloys can lead to a deterioration of their coercivity due to the increasing surface to volume ratio. Such an effect was observed experimentally. The motioned in introduction Tb–Fe–Nb–B alloy lost coercivity as grains with average diameter below 1 μm [20]. It seems that the occurrence of higher surface to volume contribution is not favorable to magnetic hardening for the systems containing high coercive phases. This is originated from the changing coercivity mechanism, i.e. the reverse magnetization process is initialized by the surface spins for which magnetic saturation occurs in lower field, comparing to the volume. If the magnetic coupling between the surface on volume is strong enough, a resultant coercivity of the whole object is decreased. Of course, if the grinding process introduces another kinds of anisotropy (via internal stresses and crystal deformations) the described effect can be opposite.

4. Conclusions

The main conclusions can be summarized as follows:

- The influence of $N_S/(N_S + N_V)$ and K_S on the anisotropy field is a complex problem and depends on a relation between K_S and K_V.
- For the objects without volume anisotropy (K_V = 0 eV), the higher values of K_S causes significant increase of the fractal anisotropy field. Simultaneously, low K_S value makes the remagnetization process more easy (the decrease of H_C) with increasing contribution of the spins on the surface.
- For the fractal with height volume anisotropy, the appearing of non-zero surface anisotropy results in magnetic softening of the whole object. Moreover, the increase of the surface contribution lead to the significant deterioration of its hard magnetic properties (i.e. decrease of H_C).
- As shown, the surface anisotropy causes non-collinear spin alignment in the surface and neighboring area. This effect leads to the situation in which some surface spins can change direction in lower external field. Finally, whole object can be remagnetized in lower field as a consequence of the exchange coupling between the surface and volume.
- If the surface anisotropy is remarkable higher than in the volume, the resultant anisotropy field reflects overall surface anisotropy.

Acknowledgement

This work was supported by National Science Centre in Poland by the grant 2015/19/B/ST8/02636.

References

[1] M. Sagawa, S. Fujimura, H. Yamamoto, Y. Matsuura, Permanent magnet materials based on the rare earth-iron-boron tetragonal compounds, IEEE Trans. Magn. 20 (5) (1984) 1584–1589.

[2] J.M.D. Coey, Permanent magnets: plugging the gap, Scr. Mater. 67 (2012) 524–529.

[3] O. Gutfleisch, Controlling the properties of high energy density permanent magnetic materials by different processing routes, J. Phys. D Appl. Phys. 33 (2000) 157–172.

[4] N. Poudyal, J. Ping Liu, Advances in nanostructured permanent magnets research, J. Phys. D Appl. Phys. 46 (2013), 043001.

[5] N. Randrianantoandro, A.D. Crisan, O. Crisan, J. Marcin, J. Kovac, J. Hanko, J. M. Grenèche, P. Svec, A. Chrobak, I. Skorvanek, The influence of microstructure on magnetic properties of nanocrystalline Fe–Pt–Nb–B permanent magnet ribbons, J. Appl. Phys. 108 (2010), 093910.

[6] A. Chrobak, G. Ziółkowski, N. Randrianantoandro, J. Klimontko, D. Chrobak, K. Prusik, J. Rak, Ultra-high coercivity of (Fe86xNbxB14)0.88Tb0.12 bulk nanocrystalline magnets, Acta Mater. 98 (2015) 318–326.

[7] G. Ziółkowski, A. Chrobak, N. Randrianantoandro, M. Kędziołka-Gaweł, J. Klimontko, Influence of transition and rare earth elements on magnetic properties of Fe-Nb-B-M (M=Ni, Ag, Gd, Tb) bulk nanocrystalline alloys, Acta Phys. Pol., A 121 (2012) 1266–1269.

[8] R. Masrour, A. Jabar, A. Benyoussef, M. Hamedoun, Magnetic properties of cluster dendrimers of core/shell with mixed spins σ = 3/2 and S = 2: a Monte Carlo study, Chem. Phys. Lett. 691 (2018) 199–205.

[9] R. Masrour, A. Jabar, Magnetic properties of dendrimer structures with different coordination numbers: a Monte Carlo study, J. Magn. Magn. Mater. 417 (2016) 397–400.

[10] A. Jabar, R. Masrour, Magnetic properties of magnetic bilayer Kekulene structure: a Monte Carlo study, Phys. B Condens. Matter 539 (2018) 21–28.

[11] A. Chrobak, G. Ziółkowski, K. Granek, et al., Disorder-based cluster Monte Carlo algorithm and its application in simulations of magnetization processes, Comput. Phys. Commun. 238 (2019) 157–164.

[12] R.H. Swendsen, J.S. Wang, Nonuniversal critical dynamics in Monte Carlo simulations, Phys. Rev. Lett. 58 (1987) 8688.

[13] U. Wolff, Collective Monte Carlo updating for spin systems, Phys. Rev. Lett. 62 (1989) 361.

[14] T.A. Witten, L.M. Sander, Diffusion-limited aggregation: a kinetic critical phenomenon, Phys. Rev. Lett. 47 (1981) 1400–1403.

[15] L.M. Sander, Fractal growth processes, Nature (1986) 322.

[16] T.A. Witten, L.M. Sander, Diffusion-limited aggregation, Phys. Rev. B 27 (1983).

[17] L.M. Sander, Z.M. Cheng, R. Richter, Diffusion-limited aggregation in three dimensions, Phys. Rev. B 28 (1983) 6394–6396.

[18] P.D. Bourke, Constrained diffusion limited aggregation in 3 dimensions, Comput. Graph. 30 (2006) 646–649.

[19] G. Herzer, Anisotropies in soft magnetic nanocrystalline alloys, J. Magn. Magn. Mater. 294 (2005) 99–106.

[20] K. Granek, G. Ziółkowski, A. Chrobak, J. Klimontko, E. Talik, Size effect of hard magnetic properties of Fe-Nb-B-Tb milled alloys, Acta Phys. Pol., A 133 (2018) 645–647.